AMERICAN SOCIETY FOR MICROBIOLOGY | Antimicrobial Agents and Chemotherapy®

EXPERIMENTAL THERAPEUTICS

Neutralizing Alpha-Toxin Accelerates Healing of *Staphylococcus aureus*-Infected Wounds in Nondiabetic and Diabetic Mice

Roger V. Ortines,[a] Haiyun Liu,[a] Lily I. Cheng,[b] Taylor S. Cohen,[c] Heather Lawlor,[c] Abhishek Gami,[a] Yu Wang,[a] Carly A. Dillen,[a] Nathan K. Archer,[a] Robert J. Miller,[a] Alyssa G. Ashbaugh,[a] Bret L. Pinsker,[a] Mark C. Marchitto,[a] Christine Tkaczyk,[c] C. Kendall Stover,[c] Bret R. Sellman,[c] Lloyd S. Miller[a,d,e,f]

[a]Department of Dermatology, Johns Hopkins University School of Medicine, Baltimore, Maryland, USA
[b]Department of Translational Science, MedImmune, LLC, Gaithersburg, Maryland, USA
[c]Department of Infectious Disease, MedImmune, LLC, Gaithersburg, Maryland, USA
[d]Department of Orthopaedic Surgery, Johns Hopkins University School of Medicine, Baltimore, Maryland, USA
[e]Department of Medicine, Division of Infectious Diseases, Johns Hopkins University School of Medicine, Baltimore, Maryland, USA
[f]Department of Materials Science and Engineering, Johns Hopkins University, Baltimore, Maryland, USA

ABSTRACT *Staphylococcus aureus* wound infections delay healing and result in invasive complications such as osteomyelitis, especially in the setting of diabetic foot ulcers. In preclinical animal models of *S. aureus* skin infection, antibody neutralization of alpha-toxin (AT), an *S. aureus*-secreted pore-forming cytolytic toxin, reduces disease severity by inhibiting skin necrosis and restoring effective host immune responses. However, whether therapeutic neutralization of alpha-toxin is effective against *S. aureus*-infected wounds is unclear. Herein, the efficacy of prophylactic treatment with a human neutralizing anti-AT monoclonal antibody (MAb) was evaluated in an *S. aureus* skin wound infection model in nondiabetic and diabetic mice. In both nondiabetic and diabetic mice, anti-AT MAb treatment decreased wound size and bacterial burden and enhanced reepithelialization and wound resolution compared to control MAb treatment. Anti-AT MAb had distinctive effects on the host immune response, including decreased neutrophil and increased monocyte and macrophage infiltrates in nondiabetic mice and decreased neutrophil extracellular traps (NETs) in diabetic mice. Similar therapeutic efficacy was achieved with an active vaccine targeting AT. Taken together, neutralization of AT had a therapeutic effect against *S. aureus*-infected wounds in both nondiabetic and diabetic mice that was associated with differential effects on the host immune response.

KEYWORDS *Staphylococcus aureus*, alpha-toxin, hla, wound, wound infection, wound healing, neutrophil, monocyte, macrophage, neutrophil extracellular traps (NETs), diabetes

Skin wounds affect more than 6 million individuals in the United States alone, which corresponds to an annual national health care burden of $25 billion (1). These numbers are expected to rise because of the aging population and the growing numbers of individuals suffering from obesity and diabetes (2, 3). In particular, 15 to 25% of diabetics will develop wounds during their lifetime, especially diabetic foot ulcers (DFU), which are often associated with peripheral neuropathy and peripheral vascular disease and complicate their treatment (4, 5). Diabetic foot ulcers precede 85% of all lower extremity amputations and are associated with a 50% higher mortality in diabetics (2, 3).

Staphylococcus aureus, an extracellular Gram-positive bacterium, is the most com-

Received 7 November 2017 **Returned for modification** 2 December 2017 **Accepted** 3 January 2018

Accepted manuscript posted online 8 January 2018

Citation Ortines RV, Liu H, Cheng LI, Cohen TS, Lawlor H, Gami A, Wang Y, Dillen CA, Archer NK, Miller RJ, Ashbaugh AG, Pinsker BL, Marchitto MC, Tkaczyk C, Stover CK, Sellman BR, Miller LS. 2018. Neutralizing alpha-toxin accelerates healing of *Staphylococcus aureus*-infected wounds in nondiabetic and diabetic mice. Antimicrob Agents Chemother 62:e02288-17. https://doi.org/10.1128/AAC.02288-17.

Address correspondence to Lloyd S. Miller, lloydmiller@jhmi.edu.

mon cause of skin and soft tissue infections in humans and is an important cause of invasive and life-threating infections such as pneumonia, osteomyelitis, and bacteremia (6, 7). Although acute and chronic wounds are most often polymicrobial and comprised of many different bacterial species, *S. aureus* is the most common bacterial pathogen associated with wound infections, and its presence correlates with significant delays in wound healing (8). Moreover, the treatment of *S. aureus* infections has been complicated by the widespread emergence of virulent and multidrug-resistant community-acquired methicillin-resistant *S. aureus* (MRSA) strains (6, 7). *S. aureus* wound infections have been reported to occur in 28 to 76% of DFU, and of these infections, the prevalence of MRSA has ranged between 12 and 30.2% (9). Osteomyelitis, a major complication in 60% of DFU, is caused by *S. aureus* in 50% of cases (10) and is exceedingly difficult to treat, as it requires prolonged antibiotic courses and surgical interventions, including debridement, resection, or amputation (2, 4, 9, 11, 12).

S. aureus possesses many virulence factors that contribute to disease severity and evasion of host immune defenses (13–15). Specifically, alpha-toxin (AT) (also called alpha-hemolysin) is a key *S. aureus* virulence factor that has been strongly associated with skin and soft tissue infections in humans (16). AT interacts with its host cell receptors ADAM10 and pleckstrin homology-containing domain 7 (PLEKHA7) to elicit its pore-forming cytolytic activity (17, 18). In mouse and rabbit *S. aureus* skin infection models, in which the bacteria are inoculated by intradermal or subcutaneous injection, AT cytolytic activity results in epidermal and dermal necrosis (16). In addition, neutralization of AT either with an anti-AT monoclonal antibody (MAb) or by active immunization strategies has been shown to decrease disease severity and restore effective innate and adaptive immune responses in these *S. aureus* skin infection models (19–26). However, whether neutralizing AT activity has a therapeutic effect against *S. aureus*-infected wounds is unknown. Therefore, we chose to investigate the preclinical efficacy of therapeutic neutralization of AT and potential mechanisms involved against *S. aureus*-infected full-thickness wounds in nondiabetic and diabetic mice.

RESULTS

Effect of neutralizing AT on *S. aureus*-infected wound resolution. To determine whether neutralization of AT has a therapeutic effect against *S. aureus*-infected skin wounds, nondiabetic mice (C57BL/6) or diabetic mice (TallyHo/JngJ mice that develop a disease resembling type 2 diabetes in humans) were passively immunized with a human anti-AT IgG1 (MEDI4893*) or an isotype control IgG (c-IgG) 1 day prior to performing a mouse model of *S. aureus* wound infection. MEDI4893* is a high-affinity, AT neutralizing MAb that reduces disease severity in mouse and rabbit *S. aureus* skin infection models and provides coverage against many clinical *S. aureus* isolates (25–28). The mouse model of *S. aureus* wound infection employed was previously described (29, 30). Briefly, three parallel 8-mm-long full-thickness scalpel wounds with approximately 1.5-mm distance between the incisions were made on the backs of the mice, and 1×10^8 CFU of a bioluminescent community-acquired MRSA strain (SAP231 [31]) was pipetted directly into the open wounds. This model was chosen because the *S. aureus* infection exacerbates wound healing, resulting in the three wounds coalescing into a single large ulcerated wound that takes longer to heal than mock-infected wounds (pipetting phosphate-buffered saline [PBS] into the wounds), which heal as individual wounds (29, 30).

In nondiabetic mice treated with c-IgG, the individual scalpel incisions coalesced into a single large wound that peaked in size on day 5 and was not healed by 14 days (Fig. 1A and B). In contrast, anti-AT MAb treatment resulted in less rapid coalescence of the incisions, significantly reduced wound sizes (similar to mock-infected wounds), and complete reepithelialization by 14 days. Diabetic mice treated with c-IgG developed a single large coalescent wound (which was substantially larger than the wound in nondiabetic mice) that peaked on day 5 and was not healed by 14 days (Fig. 1C and D). Anti-AT MAb treatment of diabetic mice also resulted in a lack of coalescence of the

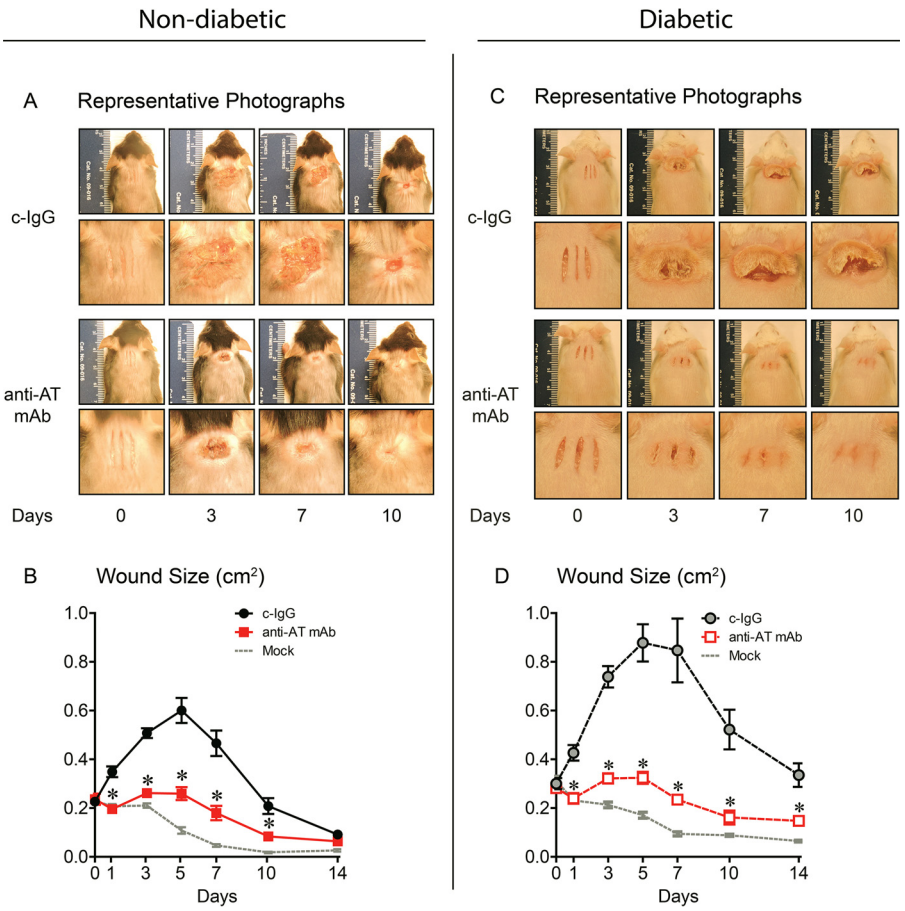

FIG 1 Neutralizing AT resulted in decreased wound sizes in nondiabetic and diabetic mice. Nondiabetic (A and B) or diabetic (C and D) mice were injected i.p. with isotype control (c-IgG) or anti-AT MAb (10 mg/kg) 1 day before performing three parallel scalpel wounds on the upper back skin and inoculation of bioluminescent *S. aureus* (10 mice in each group). Mock-infected mice were wounded but not infected. (A and C) Representative photographs of the wounds (top rows) with close-ups (bottom rows). (B and D) total wound size (in square centimeters). Values are means ± standard errors of the means (SEM) (error bars). Values for mice given anti-AT MAb that are significantly different ($P < 0.05$) from the values for mice given the isotype c-IgG by Student's *t* test (two-tailed, unpaired) are indicated by an asterisk.

individual scalpel incisions, significantly decreased wound sizes (similar to mock-infected wounds), and complete reepithelialization by 14 days.

Impact of neutralizing AT on bacterial burden. To measure bacterial burden, *in vivo* bioluminescence imaging (BLI), which noninvasively measures light production of live and actively metabolizing bioluminescent bacteria in the wound, was performed longitudinally over the course of the experiment. These data were confirmed with *ex vivo* CFU enumeration of homogenized skin wounds obtained at specific time points. In nondiabetic mice, anti-AT MAb treatment significantly decreased BLI signals on days 1 and 3 and *ex vivo* CFU on days 7 and 10 after wounding and infection compared with c-IgG (Fig. 2A to C). In diabetic mice, anti-AT MAb significantly decreased BLI signals on days 3, 5, and 7 and *ex vivo* CFU on days 3 and 7 after wounding and infection compared with c-IgG (Fig. 2D to F). Therefore, in addition to decreasing wound sizes, anti-AT neutralization decreased bacterial burdens in the wounds in both nondiabetic and diabetic mice.

Neutralizing AT promoted reepithelization and healing in nondiabetic and diabetic mice. Histologic sections from nondiabetic and diabetic mice on days 3 and 7 following wounding and infection were evaluated to determine whether AT neutralization promoted wound healing. On day 3, c-IgG-treated nondiabetic mice had full-thickness necrosis of all skin layers with bacterial clusters within an abscess in the

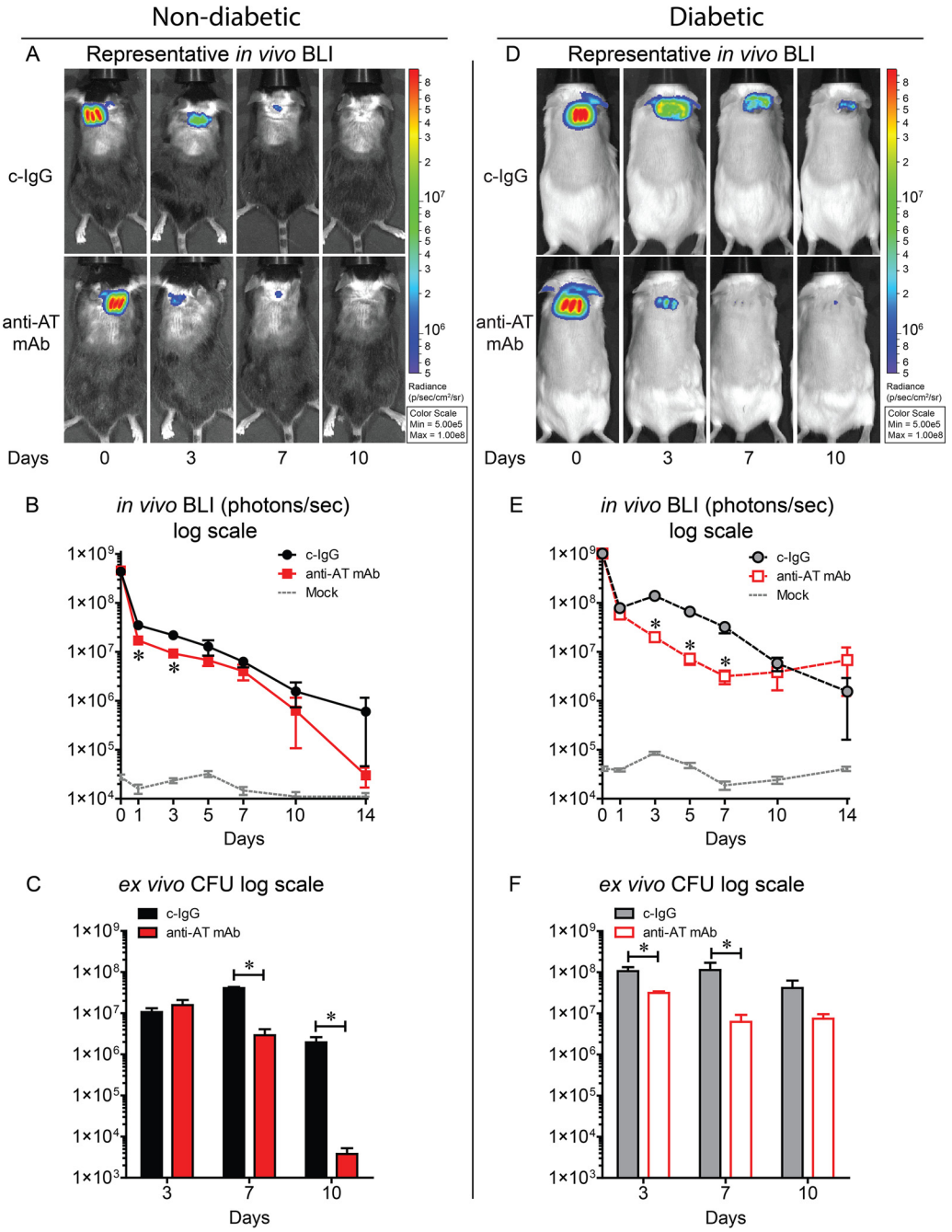

FIG 2 Neutralizing AT resulted in decreased bacterial burden in nondiabetic and diabetic mice. Nondiabetic (A to C) or diabetic (D to F) mice were injected i.p. with isotype control (c-IgG) or anti-AT MAb (10 mg/kg) 1 day prior to performing three parallel scalpel wounds on the upper back skin and inoculation of bioluminescent *S. aureus* (10 mice in each group). Mock-infected mice were wounded but not infected. (A and D) Representative *in vivo* bioluminescence imaging (BLI) signals on a color scale overlaid on a gray-scale photograph of the mice. (B and E) Mean total flux (in photons per second) ± SEM (logarithmic scale). (C and F) Mean *ex vivo* CFU ± SEM isolated from 10-mm punch biopsy specimens performed on euthanized mice at the indicated time points (logarithmic scale). Values for mice given anti-AT MAb that are significantly different ($P < 0.05$) from the values for mice given the isotype c-IgG by Student's *t* test (unpaired, two-tailed test [B and E] or one-tailed[C and F]) are indicated by an asterisk.

dermis and subcutis spanning almost the entire width of the section (Fig. 3A). In contrast, anti-AT MAb-treated nondiabetic mice demonstrated three relatively distinct sites of abscess formation with bacterial clusters localized to the scalpel wound sites and maintained an intact epidermis (with mild epidermal hyperplasia) between the scalpel incisions (Fig. 3B). In the diabetic mouse model, c-IgG-treated skin sections

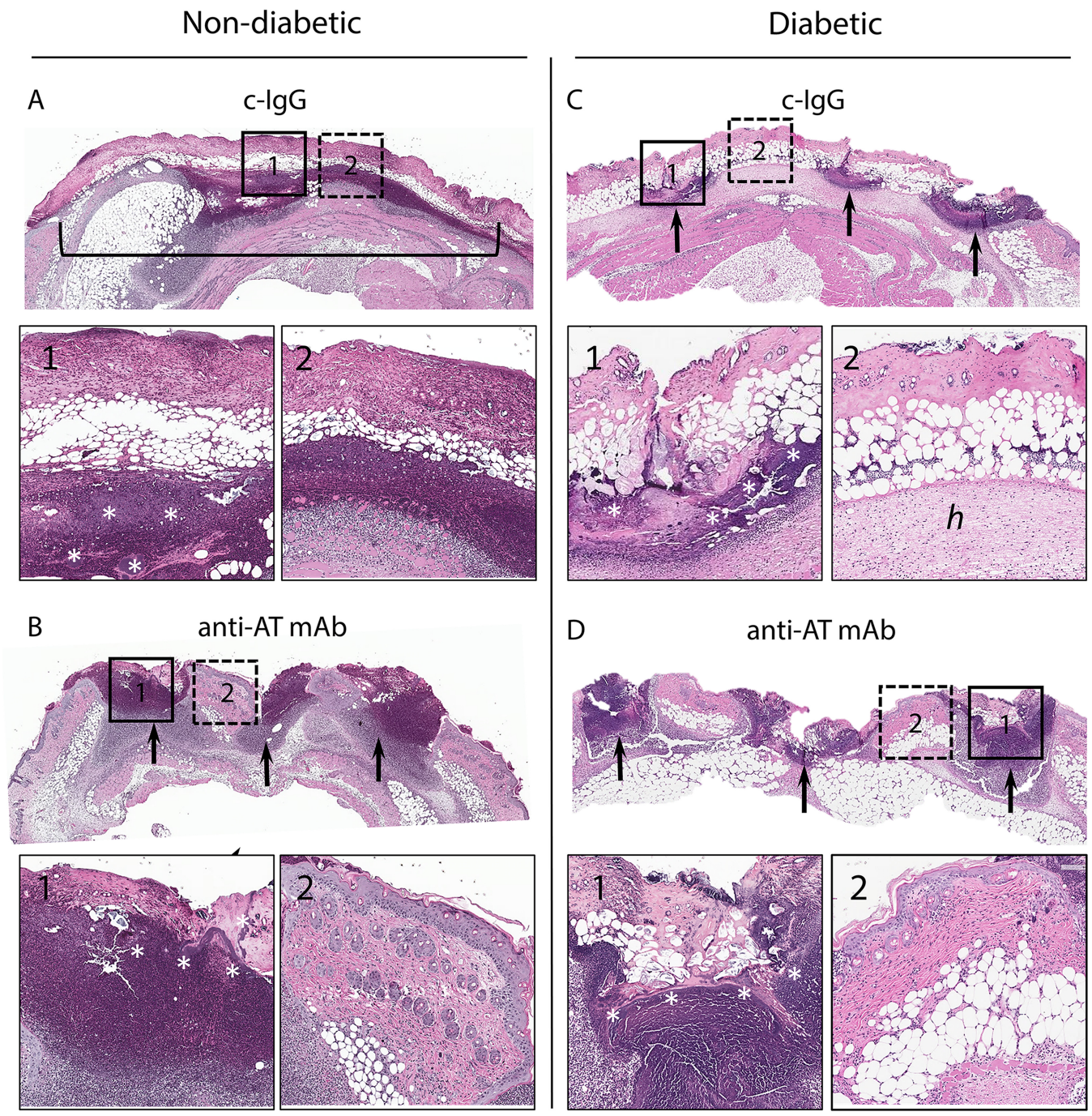

FIG 3 Representative hematoxylin and eosin histology on day 3. Nondiabetic (A and B) or diabetic (C and D) mice were injected i.p. with isotype c-IgG or anti-AT MAb (10 mg/kg) 1 day prior to performing three parallel scalpel wounds on the upper back skin and inoculation of *S. aureus* (the three mice in each group gave similar results). Low-magnification views of skin section (2× magnification) with insets indicating the site of the wound (insets 1 with solid outline and 10× magnification) and area between wound sites (insets 2 with dotted outline and 10× magnification). The black bracket in panel A shows a single coalesced ulcer with necrosis of all skin layers. Black arrows in panels B, C, and D point to wound sites. In panel C2, hypodermis with edema (*h*) is indicated. The white asterisks in panels A1, B1, C1, and D1 indicate bacterial clusters.

demonstrated less demarcated abscesses at the sites of the scalpel wound but diffuse necrosis of all skin layers that spanned almost the entire width of the section with many bacterial clusters and marked edema of the hypodermis (Fig. 3C). Anti-AT MAb-treated diabetic mice had histologic findings similar to the anti-AT MAb-treated nondiabetic mice but with more abundant bacterial clusters (consistent with the higher bacterial burden in Fig. 2D to F) and smaller abscess formation between intact areas of mildly thickened skin (Fig. 3D).

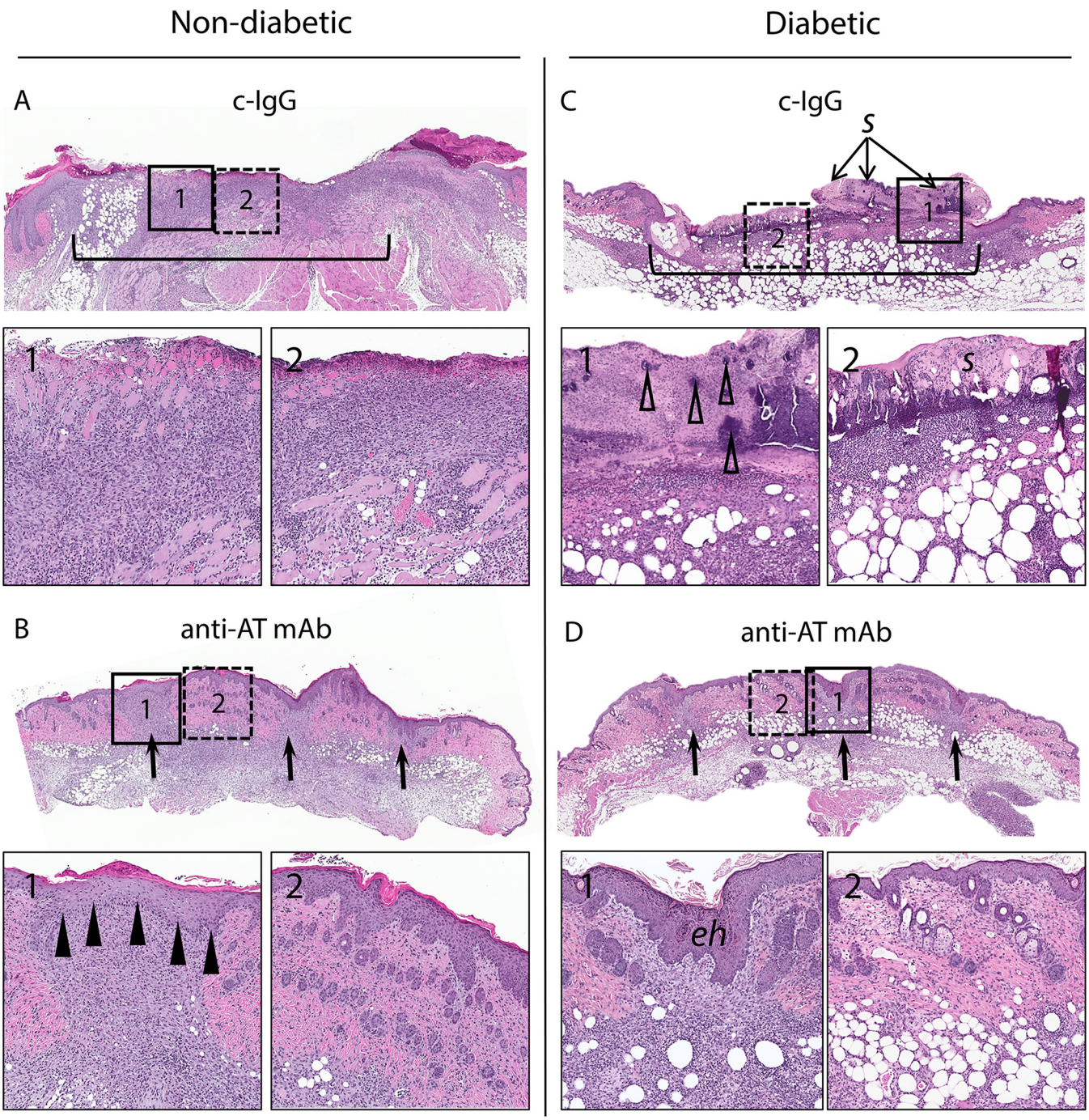

FIG 4 Representative hematoxylin and eosin histology on day 7. Nondiabetic (A and B) or diabetic (C and D) mice were injected i.p. with a matched isotype c-IgG or anti-AT MAb (10 mg/kg) 1 day prior to performing three parallel scalpel wounds on the upper back skin and inoculation of *S. aureus* (three mice in each group gave similar results). Low-magnification views of skin section (2× magnification) with insets indicating the site of the wound (insets 1 with solid outline and 10× magnification) and area between wound sites (insets 2 with dotted outline and 10× magnification). The black brackets in panels A and C show a single coalesced ulcer with diffuse dermal infiltrate. Black arrows in panels B and D point to wound sites. Black arrowheads in panel B1 indicate reepithelialization at the wound site. Open arrowheads in panel C1 indicate bacterial clusters. Serocellular crust (*s*) in panel C2 and epidermal hyperplasia (*eh*) in panel D1 are indicated.

On day 7, c-IgG-treated nondiabetic mice had diffuse loss of the epidermis spanning almost the entire width of the section with marked inflammatory infiltrates extending to the base of the ulcer in the dermis and subcutis (Fig. 4A). In contrast, anti-AT MAb-treated nondiabetic mice had complete reepithelialization and an inflammatory infiltrate at the incision sites (Fig. 4B). c-IgG-treated diabetic mice had an ulcer spanning

almost the entire width of the section with a thick serocellular crust overlying full-thickness necrosis and inflammation of the all skin layers with abundant bacterial clusters but evidence of reepithelialization on the periphery of the wound (Fig. 4C). The histologic findings for anti-AT MAb-treated diabetic mice were similar to the findings for the anti-AT MAb-treated nondiabetic mice with complete reepithelialization and mild dermal inflammatory infiltrates at the residual incision sites. The skin between incision sites had minimal dermal infiltrates but otherwise normal adenexal structures (Fig. 4D). Collectively, in *S. aureus*-infected wounds of both nondiabetic and diabetic mice, neutralizing AT preserved the epidermis between the scalpel wounds that resulted in more rapid reepithelialization and wound healing.

Neutralizing AT decreased neutrophil and increased monocyte and macrophage infiltrates in nondiabetic mice but not in diabetic mice. To determine whether AT neutralization resulted in differences in the cellular composition of the immune cell infiltrates in the wounds of nondiabetic and diabetic mice, the numbers and percentages of neutrophils ($Ly6G^{high}$), monocytes ($Ly6C^{high}$, $Ly6G^{low}$) and macrophages ($F4/80^{+}$, $Ly6G^{neg}$) were determined by fluorescence-activated cell sorting (FACS) analysis on skin wound samples obtained on days 3 and 7 (Fig. 5). On day 3, in comparing anti-AT MAb- and c-IgG-treated nondiabetic mice, there were no differences in the numbers and percentages of neutrophils, monocytes, or macrophages (Fig. 5A to H). However, on day 7, anti-AT MAb-treated nondiabetic mice had decreased numbers and percentages of neutrophils but increased numbers and percentages of monocytes and an increased percentage of macrophages. In contrast, in comparing anti-AT MAb- and c-IgG-treated diabetic mice on day 3 or 7, there were no differences in the numbers or percentages of neutrophils, monocytes, or macrophages (Fig. 5I to P). These results suggest that the anti-AT MAb impacted neutrophil, monocyte, and macrophage infiltrates in nondiabetic mice but not in diabetic mice.

Neutralizing AT inhibited formation of NETs in diabetic mice. Neutrophils are innate immune cells important for the early inflammatory phase of wound healing. As part of their antibacterial defense mechanism, they can produce neutrophil extracellular traps (NETs), through a process called NETosis, by releasing decondensed chromatin and intragranular proteases (32). Previously, NETosis was reported to be prevalent in diabetic wounds in both mouse models and in humans and contributed to aberrant inflammation that delayed wound healing (33, 34). To determine whether AT neutralization resulted in differences in NETosis, histologic sections from nondiabetic and diabetic mice on day 7 were labeled with anti-Ly6G (neutrophils) and anti-histone H3 antibodies (Fig. 6). Anti-AT MAb- or c-IgG-treated nondiabetic mice showed almost no NET formation (Fig. 6A and B). In contrast, there was marked NETosis in c-IgG-treated diabetic mice as indicated by diffuse histone H3 labeling (Fig. 6C and D). However, the anti-AT neutralizing MAb almost entirely inhibited NETosis as evidenced by markedly less histone H3 labeling.

Neutralization of AT with an active vaccine accelerates *S. aureus*-infected wound resolution. Next, we assessed whether active immunization with a nontoxigenic AT (AT with an H-to-L change at position 35 [AT_{H35L}]) in alum could exhibit protection similar to the anti-AT MAb. Active immunization with AT_{H35L} resulted in decreased wound sizes and bacterial burdens in both nondiabetic and diabetic mice compared to PBS-immunized animals (Fig. 7A to D). Thus, neutralization of AT with either an anti-AT MAb or active vaccine targeting AT had a similar therapeutic effect in promoting wound healing and decreasing bacterial burden in nondiabetic and diabetic mice.

DISCUSSION

S. aureus is the most common bacterial pathogen that infects acute and chronic wounds, leading to delayed wound healing and invasive complications such as osteomyelitis, particularly in the setting of diabetes (2, 4, 9, 11, 12). In the present study, we evaluated whether neutralization of AT provided a therapeutic benefit in an *S. aureus* wound infection mouse model. We report that passive immunization of both nondia-

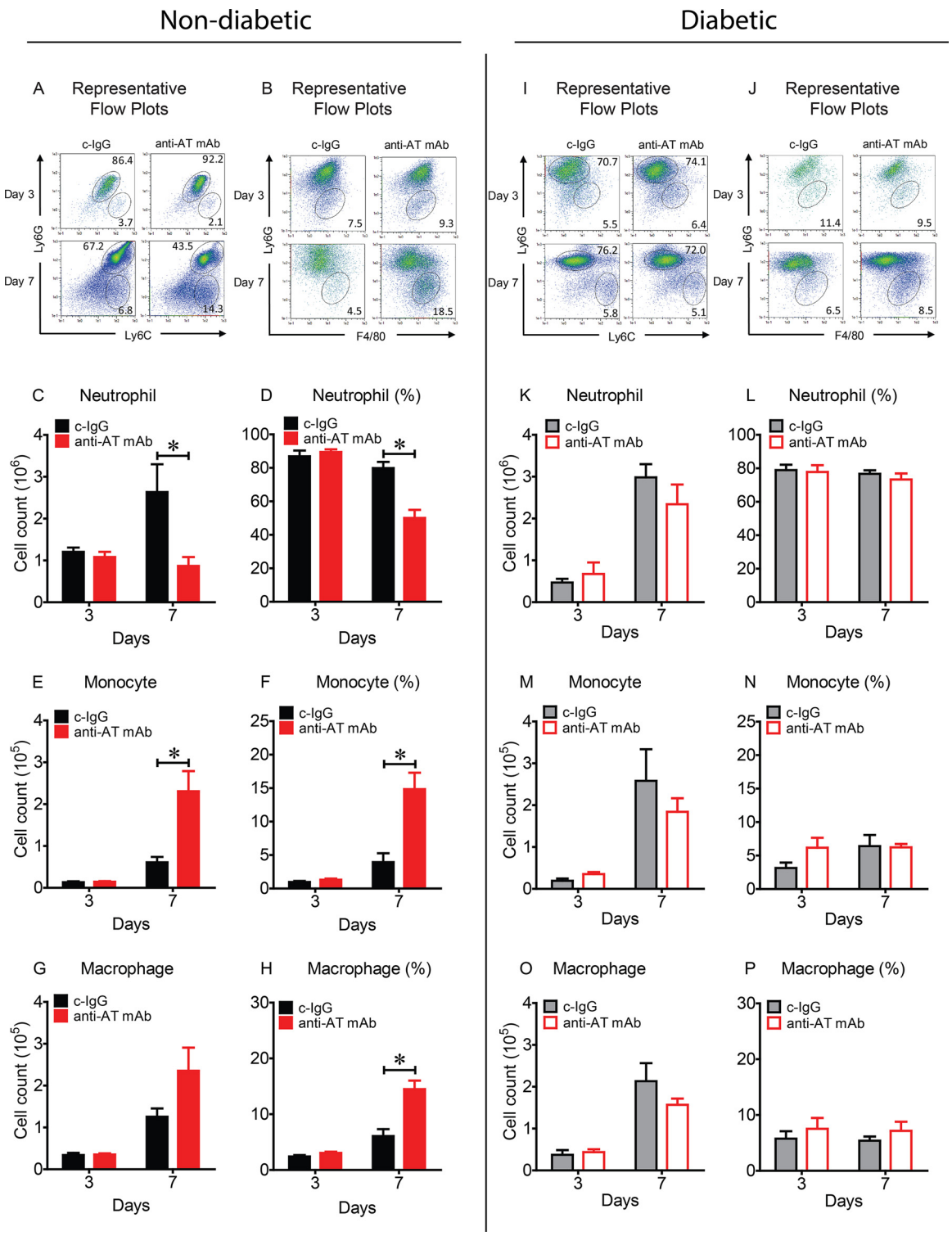

FIG 5 Neutralizing AT resulted in decreased neutrophil and increased monocyte and macrophage infiltrates in nondiabetic mice but not in diabetic mice. Nondiabetic (A to H) or diabetic (I to P) mice were injected i.p. with isotype c-IgG or anti-AT MAb (10 mg/kg) 1 day prior to performing three parallel scalpel wounds on the upper back skin and inoculation of *S. aureus* (10 mice in each group). (A, B, I, and J) Representative flow plots from *S. aureus*-infected wounds on day 3 and day 7. Total cell numbers and percentage of $CD11b^{+}$ cells of neutrophils ($Ly6G^{high}$) (C, D, K, and L), monocytes ($Ly6C^{high}$ $Ly6G^{low}$) (E, F, M, and N) and macrophages ($F4/80^{+}$, $Ly6G^{neg}$) (G, H, O, and P). Values that are significantly different ($P < 0.05$) by Student's *t* test (two tailed, unpaired) are indicated by a bar and asterisk.

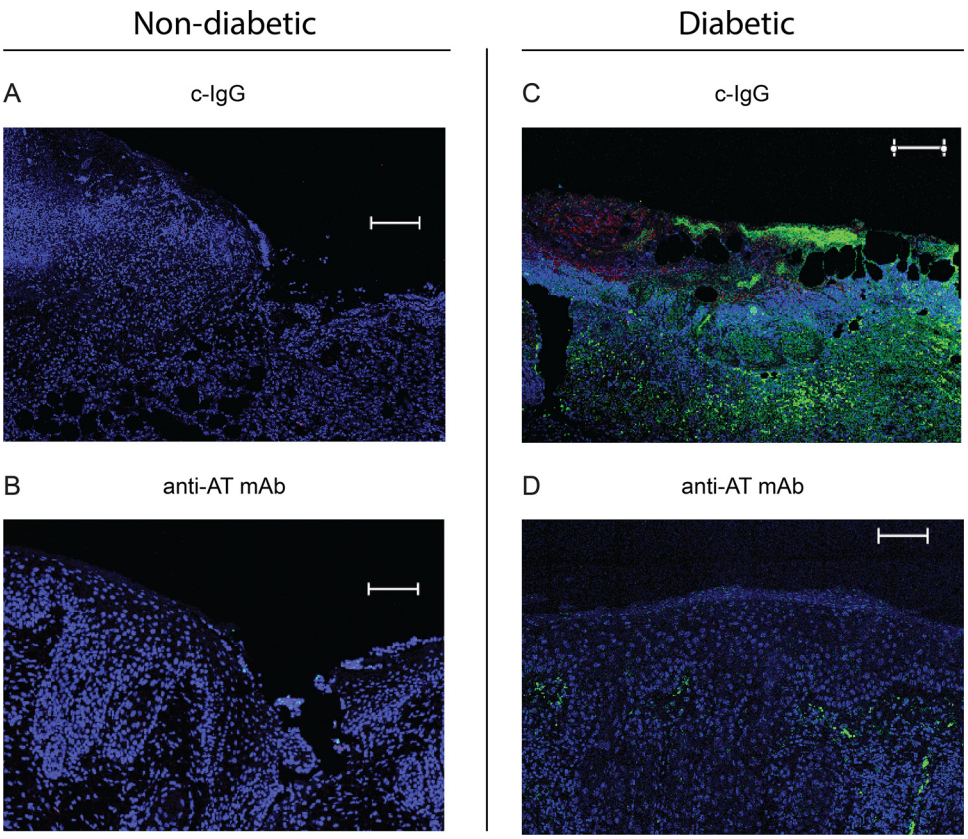

FIG 6 Neutralizing AT resulted in decreased neutrophil extracellular traps (NETs) in diabetic mice. Nondiabetic (A and B) or diabetic (C and D) mice were injected i.p. with isotype c-IgG or anti-AT MAb (10 mg/kg) 1 day prior to performing three parallel scalpel wounds on the upper back skin and inoculation of *S. aureus*, and wound biopsy specimens were taken on day 7 for immunofluorescence microscopy (the three mice in each group gave similar results). Representative immunofluorescence labeling of anti-histone H3 antibodies (NETs [green fluorescence]), anti-Ly6G antibodies (neutrophils [red fluorescence]), and DAPI stain (DNA [blue fluorescence]). Bars = 100 μm (DAPI staining).

betic and diabetic mice with an AT neutralizing MAb resulted in markedly reduced wound sizes, shorter duration to complete wound healing, decreased bacterial burdens, and preservation of intact epidermis compared to treatment with an isotype control MAb (c-IgG). In addition, in nondiabetic mice, neutralizing AT decreased numbers of neutrophils but increased monocytes and macrophages. In diabetic mice, neutralizing AT decreased formation of NETs. Finally, the efficacy of active AT vaccine was similar to that of the anti-AT MAb but with a more substantial reduction in bacterial burden in diabetic mice than in nondiabetic mice. However, several observations suggest that the mechanisms of AT neutralization differed between nondiabetic and diabetic mice.

First, our wound model proved to be a unique system to assess the impact of AT neutralization on the keratinocytes, as it allowed examination of the epidermal viability between the three scalpel wounds. In the presence of AT activity, the *S. aureus* infection caused the individual scalpel wounds to coalesce to form a large ulcer in nondiabetic and diabetic mice, modeling the effect of *S. aureus* infection in worsening and delaying wound healing (8). In contrast, neutralizing AT activity preserved viable epithelium between the scalpel wounds that likely was responsible for more rapid reepithelialization. The microscopic preservation of the epithelium was also more clearly observed in the representative photographs of diabetic mice than nondiabetic mice (Fig. 1A and C).

Second, neutrophil recruitment is considered to play an important role in host defense against *S. aureus* infections (35). However, uncontrolled neutrophilic inflammation can lead to pathogenic tissue injury (35–37). Neutralizing AT in nondiabetic

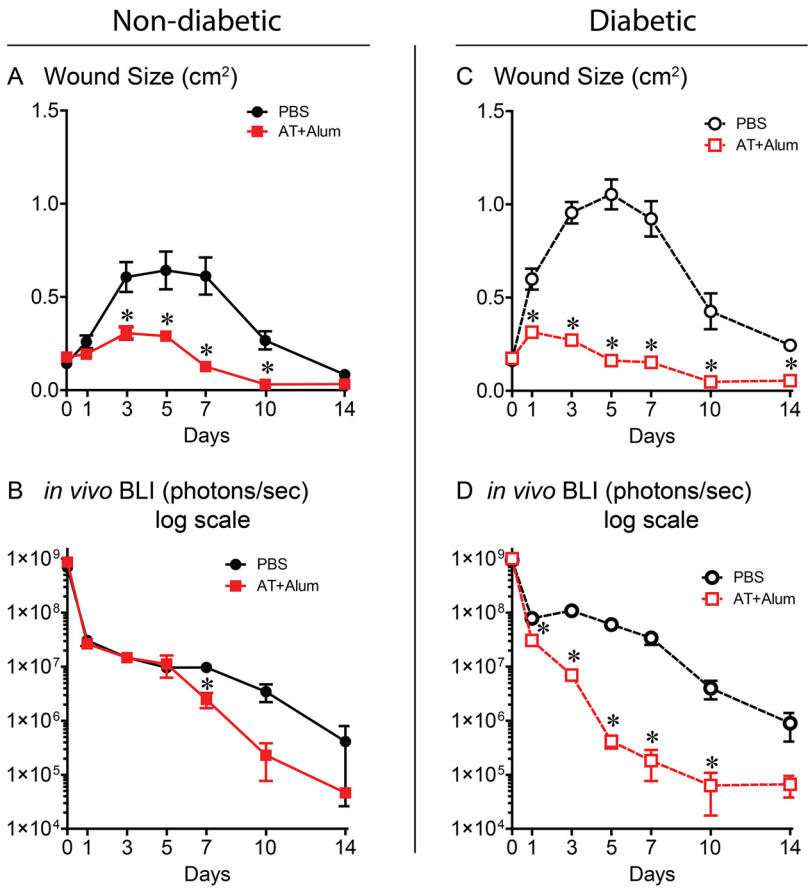

FIG 7 Neutralizing AT activity elicited by active immunization resulted in decreased wound sizes and bacterial burdens in nondiabetic and diabetic mice. Nondiabetic (A and B) or diabetic (C and D) mice were administered two doses of an active AT vaccine with alum as an adjuvant or PBS (control group) prior to performing three parallel scalpel wounds on the upper back skin and inoculation of bioluminescent *S. aureus* (five mice in each group; data are representative of two independent experiments). (A and C) Mean total wound size (cm^2) ± SEM. (B and D) Mean total flux (photons/s) ± SEM (logarithmic scale). Values for the group given AT vaccine plus alum that are significantly different ($P < 0.05$) from the value for the PBS control group by Student's *t* test (two tailed, unpaired) are indicated by an asterisk.

mice resulted in localization of the neutrophilic abscess at the wound sites and fewer neutrophils on day 7 compared with c-IgG-treated nondiabetic mice. The localization and decreased numbers of neutrophils likely resulted in less inflammation to facilitate more rapid wound healing. Although the mechanism by which neutralizing AT led to less neutrophil recruitment is not entirely clear, it could have been due to decreasing AT activation of the NLRP3/ASC inflammasome that processes pro-interleukin-1β (pro-IL-1β) to active IL-1β (38–42), which is essential for mediating neutrophil recruitment to a site of *S. aureus* infection in the skin (41).

Third, unlike nondiabetic mice, anti-AT MAb-treated diabetic mice had no differences in the numbers or percentages of neutrophils. Although the reason for this difference is unclear, neutrophil function is impaired in the setting of diabetes (43), and thus, diabetic mice are likely to have a different neutrophilic response than nondiabetic mice. Indeed, unlike nondiabetic mice, c-IgG-treated diabetic mice had substantial NETosis in the *S. aureus*-infected wounds, which is consistent with prior reports (33, 34). However, neutralizing AT almost completely inhibited NETosis, suggesting that AT neutralization might represent a new therapeutic intervention to inhibit NETosis in diabetic wounds and facilitate wound healing. This might have important clinical relevance in diabetic wounds in humans, because the increased NETosis in diabetic wounds induces aberrant inflammation that delays wound healing (33).

Fourth, in nondiabetic mice, neutralizing AT resulted in increased numbers and/or

percentages of monocytes and macrophages in the infected wounds. Although the functional consequences of this are unclear, perivascular macrophages can mediate the initial neutrophil extravasation to a site of *S. aureus* skin infection, and AT has been shown to lyse these macrophages and prevent this response (44). Thus, neutralizing AT might have prevented cell death of these macrophages to sustain early neutrophil recruitment to control the infection. Macrophages also engulf and digest apoptotic neutrophils in a process called efferocytosis to decrease neutrophilic inflammation and promote wound healing (45). We previously found that sublytic levels of AT impaired the ability of macrophages to take up apoptotic neutrophils, and the presence of AT reduced the uptake of neutrophils by macrophages in an *S. aureus* pneumonia model *in vivo* (46). Thus, the increased macrophages in anti-AT MAb-treated mice might have led to enhanced efferocytosis of neutrophils to resolve the inflammation and promote wound healing.

Our results are consistent with previous studies that investigated neutralization of AT with an anti-AT MAb, an active vaccine against AT, or an *S. aureus* AT deletion mutant (ΔAT) in mouse models in which *S. aureus* was inoculated intradermally or subcutaneously into intact mouse skin, as all these studies reported decreased skin lesion sizes (i.e., dermonecrosis) (19–26) and some also reported decreased bacterial burdens (20, 23, 25). Also, similar to our results, a previous study using a ΔAT deletion mutant in an *S. aureus*-infected excisional punch biopsy wound model in nondiabetic mice reported enhanced wound healing and decreased bacterial burden (47). However, in a prior intradermal *S. aureus* infection, anti-AT MAb treatment increased IL-1β levels and enhanced neutrophil infiltration at the infection site (25). In contrast, in our incisional wound model and in the prior excisional wound model, neutralization of AT decreased IL-1β levels, but there was decreased and increased neutrophil infiltrates (47), respectively. Although the reasons for these differences are unclear, they were likely due to differential responses inherent to the various *S. aureus* skin and wound infection models, including cytokine responses (especially in the setting of diabetes) and the *S. aureus* strains that were used (NRS384 in the present study versus SF8300 [25] and SH1000 [47]).

Finally, the anti-AT MAb (MEDI4893*) used in this study was engineered with M252Y/S254T/T256E (YTE) mutations in its Fc region for extended serum half-life (MEDI4893), which was determined to be 80 to 112 days in healthy volunteers (48). Given our results and this relatively long half-life in humans, it might be most feasible for MEDI4893 to be used at an early stage of DFU formation such as when there is intact skin or a superficial ulceration (without evidence of infection) as prophylaxis against an ensuing *S. aureus* infection. Although not formally tested in this study, MEDI4893 could potentially be used as an adjunctive treatment modality along with medical and surgical therapy during later stages when there is a culture-positive *S. aureus* infection of more invasive DFU tracking to tendon, joint, and bone or in the presence of *S. aureus* osteomyelitis. Additional preclinical and clinical studies are needed to determine whether MEDI4893 has therapeutic efficacy in these more complicated and invasive DFU.

There are some limitations. First, the effect of neutralizing AT in the polymicrobial wound environment of most diabetic foot ulcers is unclear; however, *S. aureus* is the major potentiator of these wounds that delays wound healing (8). Second, although almost all *S. aureus* skin isolates express AT, neutralization of AT will not be a successful approach for strains that do not produce AT. Third, Panton-Valentine leukocidin (PVL) is a cytolytic toxin that has been shown to induce dermonecrosis only in humanized mice upon *S. aureus* intradermal challenge (49). Other *S. aureus* cytolytic toxins and leukocidins also have species selectivity, and these bacterial factors as well as differences in host responses between humans and mice should be taken into account when translating our results to humans (50, 51). Last, in comparison to the anti-AT MAb, the efficacy of active AT vaccine was likely due to a polyclonal antibody response against AT as well as induction of T cell responses, which will be investigated in future work.

In conclusion, neutralizing AT greatly accelerated wound resolution and had less effect on decreasing bacterial burden in both nondiabetic and diabetic mice. Our results suggest that additional preclinical testing and consideration of AT neutralization

as an adjunctive therapeutic approach for *S. aureus*-infected wounds in humans are warranted. Furthermore, the particular efficacy of neutralizing AT in diabetic mice suggests that this approach might be effective against DFU to promote wound healing and prevent osteomyelitis and other infectious complications.

MATERIALS AND METHODS

***Staphylococcus aureus* strain.** The bioluminescent *S. aureus* strain SAP231 was used in all experiments, which was generated as previously described from the wild-type parent NRS384 strain (31), a USA300 community-acquired methicillin-resistant *S. aureus* (CA-MRSA) isolate from a major skin and soft tissue outbreak in the Mississippi prison system. The SAP231 strain possesses a stably integrated modified *luxABCDE* operon from the bacterial insect pathogen *Photorhabdus luminescens*. Live and metabolically active SAP231 bacteria constitutively emit a blue-green light, which is maintained in all progeny without selection.

Preparation of bacteria for inoculation. *S. aureus* strain SAP231 was streaked onto tryptic soy agar plates and grown overnight. To obtain mid-logarithmic-phase bacteria, single colonies were selected and grown in tryptic soy broth at 37°C in a shaking incubator overnight and then subcultured for 2 h, pelleted, washed, and resuspended at an inoculum concentration of 1×10^8 CFU per 10 μl phosphate-buffered saline (PBS) estimated by absorbance (A_{600}) and verified by overnight culture on plates.

Mice. Seven- to 8-week-old male wild-type (nondiabetic) C57BL/6 mice or 8- to 9-week-old male TallyHo/JngJ mice (Jackson Laboratories, Bar Harbor, ME) were used in all experiments. TallyHo/JngJ mice were used as a model of type II diabetes and were confirmed to have hyperglycemia (blood glucose level of >300 mg/dl) before use in experiments, which occurred when the mice were between 8 and 9 weeks of age. Mice were bred and maintained under specific-pathogen-free conditions at an American Association for the Accreditation of Laboratory Animal Care (AAALAC)-accredited animal facility at Johns Hopkins and housed according to procedures described in the *Guide for the Care and Use of Laboratory Animals* (52).

Wound infection model. All animal experiments were approved by the Johns Hopkins University Animal Care and Use Committee. The *S. aureus* wound infection model was used as previously described (29, 30). Briefly, mice were anesthetized with 2% isoflurane, the back skin was shaved with clippers, and three parallel 8-mm full-thickness cuts with ~1.5 mm space between each cut on the upper dorsal back skin were made with a no. 11 blade, and the wounds were collectively inoculated with *S. aureus* at 1×10^8 CFU per 10 μl PBS using a micropipette. Wound area measurements were obtained from digital photographs by using the image analysis software ImageJ (https://imagej.nih.gov/ij/; NIH Research Services Branch) and a millimeter ruler.

Anti-AT prophylactic treatment. Human anti-alpha toxin (anti-AT) monoclonal antibody (MAb) (MEDI4893*) or isotype control IgG1 (c-IgG) (anti-HIV gp120 [R347]) was generated as previously described (26). Mice were treated with 10 mg of either MAb per kg of body weight intraperitoneally (i.p.) 1 day prior to wounding and bacterial inoculation. This dose of anti-AT MAb was chosen because in our pilot dose-finding experiments, 10 mg/kg was more efficacious in the *S. aureus* wound infection model than lower doses (2 and 0.5 mg/kg) (data not shown), and it was the same effective dose we used to inhibit AT in our prior work in an intradermal *S. aureus* infection model (25).

***In vivo* bioluminescence imaging.** Mice were anesthetized (2% isoflurane), and *in vivo* bioluminescence imaging (BLI) was performed at the indicated time points using the Lumina III IVIS *in vivo* imaging system (PerkinElmer). The total flux (in photons per second) was measured within a 1×10^3 pixel circular region of interest using Living Image software (PerkinElmer) (limit of detection, 2×10^4 photons/s).

***Ex vivo* CFU enumeration.** Mice were euthanized on days 3, 7, and 10 after the mice were wounded and infected, and 10-mm skin punch biopsy specimens were obtained and homogenized (Pro200 Series homogenizer; Pro Scientific, Oxford, CT) in PBS on ice. Homogenates were serially diluted and cultured on tryptic soy agar (TSA) plates overnight, and CFU were enumerated. In our prior work using this same *S. aureus* skin wound infection model in nondiabetic mice, the *in vivo* BLI signals showed a high correlation with the *ex vivo* CFU counts ($R^2 = 0.9996$) (30).

Histology. Mice were euthanized on day 3 and day 7 postwounding and infection. Skin specimens were obtained using surgical scissors, and specimens were fixed in 10% formalin. The samples were embedded in paraffin, then sectioned at 4-μm thickness, and mounted on glass slides for staining with hematoxylin and eosin (H&E). Histologic sections were evaluated by light microscopy by a pathologist who was blind to the experimental groups, and the histologic features that were consistent among the mice in each group are shown in the representative histologic images shown in the figures.

Flow cytometry. Mice were euthanized on day 3 and day 7 after the mice were wounded and infected, and a 10-mm punch biopsy specimen of the wounded and infected skin was obtained from euthanized mice. Skin tissue was minced with surgical scissors and digested in RPMI 1640 medium with 0.25% Liberase TL (Roche) and 0.01% DNase I (MilliporeSigma) for 2 h in an orbital shaking incubator at 70 rpm and 37°C. Samples were passed through sterile 40-μm cell strainers (Corning), and single-cell suspensions were resuspended in RPMI 1640 medium containing 10% fetal bovine serum (FBS) and penicillin-streptomycin and then washed twice in fluorescence-activated cell sorting (FACS) buffer (PBS with 1% bovine serum albumin). Approximately 1 million cells were added to each well of a 96-well plate and Fc block (BioLegend) was added, and the cells were labeled for 15 min at 4°C with propidium iodide (Miltenyi Biotec) for viability and MAbs against CD11b (clone M1/70), Ly6C (clone AL-21), Ly6G (clone 1A8) (BD Biosciences), and F4/80 (clone REA126) (Miltenyi Biotec). Cells were washed twice with FACS buffer and resuspended for data acquisition on a MACSQuant flow cytometer (Miltenyi Biotec). Data were analyzed with FlowJo software (Treestar).

Immunofluorescence and confocal laser microscopy. Paraffin-embedded tissue specimens were rehydrated by incubation in 100% xylene for 20 min followed by 5-min incubations in 100%, 90%, 75%, and 50% ethanol (EtOH). The slides were then washed in PBS prior to antigen retrieval at 95°C in 10 mM sodium citrate (20 min). Tissue sections were blocked (1 h) in BlockAid (Thermo Fisher Scientific) and stained overnight at 4°C with anti-Ly6G (clone 1A8; BD Biosciences) and anti-histone H3 (citrulline R2 plus R8 plus R17) antibodies (ab5103; Abcam), followed by Alexa Fluor 647- and Alexa Fluor 488-conjugated secondary antibodies targeting anti-rat IgG and anti-rabbit IgG, respectively (Thermo Fisher Scientific). The slides were sealed with Vectashield with 4′,6′-diamidino-2-phenylindole (DAPI) (Vector Laboratories) and imaged with a Leica TCS SP5 X confocal microscope (Leica Microsystems).

Active immunization with nontoxigenic AT mutant. Active vaccination was performed using recombinant, nontoxigenic AT (AT_{H35L}) as previously described (26) in the mouse model of wound infection using both C57BL6/J and Tallyho/JngJ mice. Vaccination was performed with intramuscular (i.m.) injection of a total of 100 μl (50 μl per hind limb) of PBS or AT_{H35L} (5 μg for C57BL6/J mice and 1 μg for Tallyho mice) in combination with alum adjuvant (Alhydrogel). C57BL6/J mice were immunized with a two-dose vaccine regimen on day 1 and day 14, and on day 28, the wound was infected as described above. Tallyho/JngJ mice were immunized with a two-dose vaccine regimen on day 1 and day 10, and on day 20, the wound was infected as described above.

Statistics. Data were compared using an unpaired Student's *t* test (one or two tailed) as indicated in the figure legends. All statistical analysis was performed using Prism v5 (GraphPad). Data are presented as means ± standard errors of the means (SEM), and values of $P < 0.05$ were considered to be statistically significant.

ACKNOWLEDGMENTS

This work was supported by a sponsored research agreement from MedImmune, LLC, through a Johns Hopkins-MedImmune Academic Industry Partnership.

The following competing financial interests are outside of this work. L.S.M. has received grant support from MedImmune, LLC, for the work reported in this article as well as grant support from Pfizer, Regeneron Pharmaceuticals, and Moderna Therapeutics and is a shareholder of Noveome Biotherapeutics, which are outside of the work reported in this article. L.I.C., T.S.C., H.L., C.T., C.K.S., and B.R.S. are associated with MedImmune, LLC, a subsidiary of AstraZeneca, and may hold AstraZeneca stock.

REFERENCES

1. Sen CK, Gordillo GM, Roy S, Kirsner R, Lambert L, Hunt TK, Gottrup F, Gurtner GC, Longaker MT. 2009. Human skin wounds: a major and snowballing threat to public health and the economy. Wound Repair Regen 17:763–771. https://doi.org/10.1111/j.1524-475X.2009.00543.x.
2. Lipsky BA, Berendt AR, Cornia PB, Pile JC, Peters EJ, Armstrong DG, Deery HG, Embil JM, Joseph WS, Karchmer AW, Pinzur MS, Senneville E, Infectious Diseases Society of America. 2012. 2012 Infectious Diseases Society of America clinical practice guideline for the diagnosis and treatment of diabetic foot infections. Clin Infect Dis 54:e132–e173. https://doi.org/10.1093/cid/cis346.
3. Uckay I, Aragon-Sanchez J, Lew D, Lipsky BA. 2015. Diabetic foot infections: what have we learned in the last 30 years? Int J Infect Dis 40:81–91. https://doi.org/10.1016/j.ijid.2015.09.023.
4. Alavi A, Sibbald RG, Mayer D, Goodman L, Botros M, Armstrong DG, Woo K, Boeni T, Ayello EA, Kirsner RS. 2014. Diabetic foot ulcers: Part II. Management. J Am Acad Dermatol 70:21.e1–21.e24. https://doi.org/10.1016/j.jaad.2013.07.048.
5. Alavi A, Sibbald RG, Mayer D, Goodman L, Botros M, Armstrong DG, Woo K, Boeni T, Ayello EA, Kirsner RS. 2014. Diabetic foot ulcers: Part I. Pathophysiology and prevention. J Am Acad Dermatol 70:1.e1–1.e18. https://doi.org/10.1016/j.jaad.2013.06.055.
6. DeLeo FR, Otto M, Kreiswirth BN, Chambers HF. 2010. Community-associated meticillin-resistant *Staphylococcus aureus*. Lancet 375:1557–1568. https://doi.org/10.1016/S0140-6736(09)61999-1.
7. Tong SY, Davis JS, Eichenberger E, Holland TL, Fowler VG, Jr. 2015. *Staphylococcus aureus* infections: epidemiology, pathophysiology, clinical manifestations, and management. Clin Microbiol Rev 28:603–661. https://doi.org/10.1128/CMR.00134-14.
8. Schierle CF, De la Garza M, Mustoe TA, Galiano RD. 2009. Staphylococcal biofilms impair wound healing by delaying reepithelialization in a murine cutaneous wound model. Wound Repair Regen 17:354–359. https://doi.org/10.1111/j.1524-475X.2009.00489.x.
9. Eleftheriadou I, Tentolouris N, Argiana V, Jude E, Boulton AJ. 2010. Methicillin-resistant *Staphylococcus aureus* in diabetic foot infections. Drugs 70:1785–1797. https://doi.org/10.2165/11538070-000000000-00000.
10. Giurato L, Meloni M, Izzo V, Uccioli L. 2017. Osteomyelitis in diabetic foot: a comprehensive overview. World J Diabetes 8:135–142. https://doi.org/10.4239/wjd.v8.i4.135.
11. Uckay I, Gariani K, Dubois-Ferriere V, Suva D, Lipsky BA. 2016. Diabetic foot infections: recent literature and cornerstones of management. Curr Opin Infect Dis 29:145–152. https://doi.org/10.1097/QCO.0000000000000243.
12. Zenelaj B, Bouvet C, Lipsky BA, Uckay I. 2014. Do diabetic foot infections with methicillin-resistant *Staphylococcus aureus* differ from those with other pathogens? Int J Low Extrem Wounds 13:263–272. https://doi.org/10.1177/1534734614550311.
13. Spaan AN, Surewaard BG, Nijland R, van Strijp JA. 2013. Neutrophils versus *Staphylococcus aureus*: a biological tug of war. Annu Rev Microbiol 67:629–650. https://doi.org/10.1146/annurev-micro-092412-155746.
14. Spaulding AR, Salgado-Pabon W, Kohler PL, Horswill AR, Leung DY, Schlievert PM. 2013. Staphylococcal and streptococcal superantigen exotoxins. Clin Microbiol Rev 26:422–447. https://doi.org/10.1128/CMR.00104-12.
15. Thammavongsa V, Kim HK, Missiakas D, Schneewind O. 2015. Staphylococcal manipulation of host immune responses. Nat Rev Microbiol 13:529–543. https://doi.org/10.1038/nrmicro3521.
16. Berube BJ, Bubeck Wardenburg J. 2013. *Staphylococcus aureus* alpha-toxin: nearly a century of intrigue. Toxins (Basel) 5:1140–1166. https://doi.org/10.3390/toxins5061140.
17. Inoshima I, Inoshima N, Wilke GA, Powers ME, Frank KM, Wang Y, Bubeck Wardenburg J. 2011. A *Staphylococcus aureus* pore-forming toxin subverts the activity of ADAM10 to cause lethal infection in mice. Nat Med 17:1310–1314. https://doi.org/10.1038/nm.2451.
18. Popov LM, Marceau CD, Starkl PM, Lumb JH, Shah J, Guerrera D, Cooper RL, Merakou C, Bouley DM, Meng W, Kiyonari H, Takeichi M, Galli SJ, Bagnoli F, Citi S, Carette JE, Amieva MR. 2015. The adherens junctions control susceptibility to *Staphylococcus aureus* alpha-toxin. Proc Natl Acad Sci U S A 112:14337–14342. https://doi.org/10.1073/pnas.1510265112.
19. Adhikari RP, Thompson CD, Aman MJ, Lee JC. 2016. Protective efficacy of a novel alpha hemolysin subunit vaccine (AT62) against *Staphylococcus*

aureus skin and soft tissue infections. Vaccine 34:6402–6407. https://doi.org/10.1016/j.vaccine.2016.09.061.
20. Brady RA, Mocca CP, Prabhakara R, Plaut RD, Shirtliff ME, Merkel TJ, Burns DL. 2013. Evaluation of genetically inactivated alpha toxin for protection in multiple mouse models of *Staphylococcus aureus* infection. PLoS One 8:e63040. https://doi.org/10.1371/journal.pone.0063040.
21. Inoshima N, Wang Y, Bubeck Wardenburg J. 2012. Genetic requirement for ADAM10 in severe *Staphylococcus aureus* skin infection. J Investig Dermatol 132:1513–1516. https://doi.org/10.1038/jid.2011.462.
22. Kennedy AD, Bubeck Wardenburg J, Gardner DJ, Long D, Whitney AR, Braughton KR, Schneewind O, DeLeo FR. 2010. Targeting of alpha-hemolysin by active or passive immunization decreases severity of USA300 skin infection in a mouse model. J Infect Dis 202:1050–1058. https://doi.org/10.1086/656043.
23. Mocca CP, Brady RA, Burns DL. 2014. Role of antibodies in protection elicited by active vaccination with genetically inactivated alpha hemolysin in a mouse model of *Staphylococcus aureus* skin and soft tissue infections. Clin Vaccine Immunol 21:622–627. https://doi.org/10.1128/CVI.00051-14.
24. Sampedro GR, DeDent AC, Becker RE, Berube BJ, Gebhardt MJ, Cao H, Bubeck Wardenburg J. 2014. Targeting *Staphylococcus aureus* alpha-toxin as a novel approach to reduce severity of recurrent skin and soft-tissue infections. J Infect Dis 210:1012–1018. https://doi.org/10.1093/infdis/jiu223.
25. Tkaczyk C, Hamilton MM, Datta V, Yang XP, Hilliard JJ, Stephens GL, Sadowska A, Hua L, O'Day T, Suzich J, Stover CK, Sellman BR. 2013. *Staphylococcus aureus* alpha toxin suppresses effective innate and adaptive immune responses in a murine dermonecrosis model. PLoS One 8:e75103. https://doi.org/10.1371/journal.pone.0075103.
26. Tkaczyk C, Hua L, Varkey R, Shi Y, Dettinger L, Woods R, Barnes A, MacGill RS, Wilson S, Chowdhury P, Stover CK, Sellman BR. 2012. Identification of anti-alpha toxin monoclonal antibodies that reduce the severity of *Staphylococcus aureus* dermonecrosis and exhibit a correlation between affinity and potency. Clin Vaccine Immunol 19:377–385. https://doi.org/10.1128/CVI.05589-11.
27. Oganesyan V, Peng L, Damschroder MM, Cheng L, Sadowska A, Tkaczyk C, Sellman BR, Wu H, Dall'Acqua WF. 2014. Mechanisms of neutralization of a human anti-alpha-toxin antibody. J Biol Chem 289:29874–29880. https://doi.org/10.1074/jbc.M114.601328.
28. Tabor DE, Yu L, Mok H, Tkaczyk C, Sellman BR, Wu Y, Oganesyan V, Slidel T, Jafri H, McCarthy M, Bradford P, Esser MT. 2016. *Staphylococcus aureus* alpha-toxin is conserved among diverse hospital respiratory isolates collected from a global surveillance study and is neutralized by monoclonal antibody MEDI4893. Antimicrob Agents Chemother 60:5312–5321. https://doi.org/10.1128/AAC.00357-16.
29. Cho JS, Zussman J, Donegan NP, Ramos RI, Garcia NC, Uslan DZ, Iwakura Y, Simon SI, Cheung AL, Modlin RL, Kim J, Miller LS. 2011. Noninvasive in vivo imaging to evaluate immune responses and antimicrobial therapy against *Staphylococcus aureus* and USA300 MRSA skin infections. J Investig Dermatol 131:907–915. https://doi.org/10.1038/jid.2010.417.
30. Guo Y, Ramos RI, Cho JS, Donegan NP, Cheung AL, Miller LS. 2013. In vivo bioluminescence imaging to evaluate systemic and topical antibiotics against community-acquired methicillin-resistant *Staphylococcus aureus*-infected skin wounds in mice. Antimicrob Agents Chemother 57:855–863. https://doi.org/10.1128/AAC.01003-12.
31. Plaut RD, Mocca CP, Prabhakara R, Merkel TJ, Stibitz S. 2013. Stably luminescent *Staphylococcus aureus* clinical strains for use in bioluminescent imaging. PLoS One 8:e59232. https://doi.org/10.1371/journal.pone.0059232.
32. Kolaczkowska E, Kubes P. 2013. Neutrophil recruitment and function in health and inflammation. Nat Rev Immunol 13:159–175. https://doi.org/10.1038/nri3399.
33. Fadini GP, Menegazzo L, Rigato M, Scattolini V, Poncina N, Bruttocao A, Ciciliot S, Mammano F, Ciubotaru CD, Brocco E, Marescotti MC, Cappellari R, Arrigoni G, Millioni R, Vigili de Kreutzenberg S, Albiero M, Avogaro A. 2016. NETosis delays diabetic wound healing in mice and humans. Diabetes 65:1061–1071. https://doi.org/10.2337/db15-0863.
34. Wong SL, Demers M, Martinod K, Gallant M, Wang Y, Goldfine AB, Kahn CR, Wagner DD. 2015. Diabetes primes neutrophils to undergo NETosis, which impairs wound healing. Nat Med 21:815–819. https://doi.org/10.1038/nm.3887.
35. Kobayashi SD, Malachowa N, DeLeo FR. 2015. Pathogenesis of *Staphylococcus aureus* abscesses. Am J Pathol 185:1518–1527. https://doi.org/10.1016/j.ajpath.2014.11.030.
36. Miller LS, Cho JS. 2011. Immunity against *Staphylococcus aureus* cutaneous infections. Nat Rev Immunol 11:505–518. https://doi.org/10.1038/nri3010.
37. Molne L, Verdrengh M, Tarkowski A. 2000. Role of neutrophil leukocytes in cutaneous infection caused by *Staphylococcus aureus*. Infect Immun 68:6162–6167. https://doi.org/10.1128/IAI.68.11.6162-6167.2000.
38. Craven RR, Gao X, Allen IC, Gris D, Bubeck Wardenburg J, McElvania-Tekippe E, Ting JP, Duncan JA. 2009. *Staphylococcus aureus* alpha-hemolysin activates the NLRP3-inflammasome in human and mouse monocytic cells. PLoS One 4:e7446. https://doi.org/10.1371/journal.pone.0007446.
39. Ezekwe EA, Jr, Weng C, Duncan JA. 2016. ADAM10 cell surface expression but not activity is critical for *Staphylococcus aureus* alpha-hemolysin-mediated activation of the NLRP3 inflammasome in human monocytes. Toxins (Basel) 8:95. https://doi.org/10.3390/toxins8040095.
40. Kebaier C, Chamberland RR, Allen IC, Gao X, Broglie PM, Hall JD, Jania C, Doerschuk CM, Tilley SL, Duncan JA. 2012. *Staphylococcus aureus* alpha-hemolysin mediates virulence in a murine model of severe pneumonia through activation of the NLRP3 inflammasome. J Infect Dis 205:807–817. https://doi.org/10.1093/infdis/jir846.
41. Miller LS, Pietras EM, Uricchio LH, Hirano K, Rao S, Lin H, O'Connell RM, Iwakura Y, Cheung AL, Cheng G, Modlin RL. 2007. Inflammasome-mediated production of IL-1beta is required for neutrophil recruitment against *Staphylococcus aureus* in vivo. J Immunol 179:6933–6942. https://doi.org/10.4049/jimmunol.179.10.6933.
42. Munoz-Planillo R, Franchi L, Miller LS, Nunez G. 2009. A critical role for hemolysins and bacterial lipoproteins in *Staphylococcus aureus*-induced activation of the Nlrp3 inflammasome. J Immunol 183:3942–3948. https://doi.org/10.4049/jimmunol.0900729.
43. Alba-Loureiro TC, Munhoz CD, Martins JO, Cerchiaro GA, Scavone C, Curi R, Sannomiya P. 2007. Neutrophil function and metabolism in individuals with diabetes mellitus. Braz J Med Biol Res 40:1037–1044. https://doi.org/10.1590/S0100-879X2006005000143.
44. Abtin A, Jain R, Mitchell AJ, Roediger B, Brzoska AJ, Tikoo S, Cheng Q, Ng LG, Cavanagh LL, von Andrian UH, Hickey MJ, Firth N, Weninger W. 2014. Perivascular macrophages mediate neutrophil recruitment during bacterial skin infection. Nat Immunol 15:45–53. https://doi.org/10.1038/nri3790.
45. Snyder RJ, Lantis J, Kirsner RS, Shah V, Molyneaux M, Carter MJ. 2016. Macrophages: a review of their role in wound healing and their therapeutic use. Wound Repair Regen 24:613–629. https://doi.org/10.1111/wrr.12444.
46. Cohen TS, Jones-Nelson O, Hotz M, Cheng L, Miller LS, Suzich J, Stover CK, Sellman BR. 2016. *S. aureus* blocks efferocytosis of neutrophils by macrophages through the activity of its virulence factor alpha toxin. Sci Rep 6:35466. https://doi.org/10.1038/srep35466.
47. Falahee PC, Anderson LS, Reynolds MB, Pirir M, McLaughlin BE, Dillen CA, Cheung AL, Miller LS, Simon SI. 2017. Alpha-toxin regulates local granulocyte expansion from hematopoietic stem and progenitor cells in *Staphylococcus aureus*-infected wounds. J Immunol 199:1772–1782. https://doi.org/10.4049/jimmunol.1700649.
48. Yu XQ, Robbie GJ, Wu Y, Esser MT, Jensen K, Schwartz HI, Bellamy T, Hernandez-Illas M, Jafri HS. 2017. Safety, tolerability, and pharmacokinetics of MEDI4893, an investigational, extended-half-life, anti-*Staphylococcus aureus* alpha-toxin human monoclonal antibody, in healthy adults. Antimicrob Agents Chemother 61:e01020-16. https://doi.org/10.1128/AAC.01020-16.
49. Tseng CW, Biancotti JC, Berg BL, Gate D, Kolar SL, Muller S, Rodriguez MD, Rezai-Zadeh K, Fan X, Beenhouwer DO, Town T, Liu GY. 2015. Increased susceptibility of humanized NSG mice to Panton-Valentine leukocidin and *Staphylococcus aureus* skin infection. PLoS Pathog 11:e1005292. https://doi.org/10.1371/journal.ppat.1005292.
50. Salgado-Pabon W, Schlievert PM. 2014. Models matter: the search for an effective *Staphylococcus aureus* vaccine. Nat Rev Microbiol 12:585–591. https://doi.org/10.1038/nrmicro3308.
51. Spaan AN, van Strijp JAG, Torres VJ. 2017. Leukocidins: staphylococcal bi-component pore-forming toxins find their receptors. Nat Rev Microbiol 15:435–447. https://doi.org/10.1038/nrmicro.2017.27.
52. National Research Council. 2011. Guide for the care and use of laboratory animals, 8th ed. National Academies Press, Washington, DC.